Check for updates

RESEARCH ARTICLE

Quantitation of Super Basic Peptides in Biological Matrices by a Generic Perfluoropentanoic Acid-Based Liquid Chromatography–Mass Spectrometry Method

Jianzhong Wen, Weixun Wang, Keun-Joong Lee, Bernard K. Choi, Paul Harradine, Gino M. Salituro, Lucinda Hittle

Pharmacokinetics, Pharmacodynamics and Drug Metabolism, Merck & Co., Inc., Rahway, NJ 07065, USA

Peptide quantitation: RRRRRRRRR
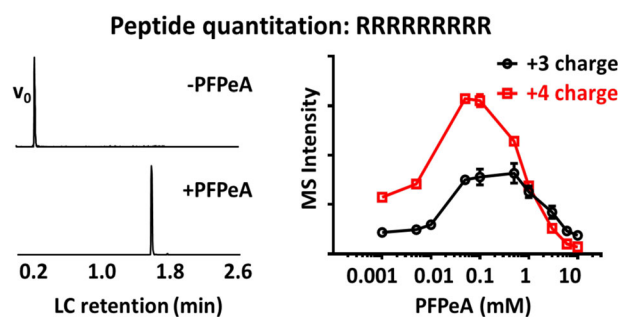
Abstract. Peptides represent a promising modality for the design of novel therapeutics that can potentially modulate traditionally non-druggable targets. Cell-penetrating peptides (CPPs) and antimicrobial peptides (AMPs) are two large families that are being explored extensively as drug delivery vehicles, imaging reagents, or therapeutic treatments for various diseases. Many CPPs and AMPs are cationic among which a significant portion is extremely basic and hydrophilic (e.g., nona-arginine). Despite their attractive therapeutic potential, it remains challenging to directly analyze and quantify these super cationic peptides from biological matrices due to their poor chromatographic behavior and MS response. Herein, we describe a generic method that combines solid phase extraction and LC-MS/MS for analysis of these peptides. As demonstrated, using a dozen strongly basic peptides, low μM concentration of perfluoropentanoic acid (PFPeA) in the mobile phase enabled excellent compound chromatographic retention, thus avoiding co-elution with solvent front ion suppressants. PFPeA also had a charge reduction effect that allowed the selection of parent/ion fragment pairs in the higher m/z region to further reduce potential low molecular weight interferences. When the method was coupled to the optimized sample extraction process, we routinely achieved low digit ng/ml sensitivity for peptides in plasma/tissue. The method allowed an efficient evaluation of plasma stability of CPPs/AMPs without fluorescence derivatization or other tagging methods. Importantly, using the widely studied HIV-TAT CPP as an example, the method enabled us to directly assess its pharmacokinetics and tissue distribution in preclinical animal models.

Keywords: Cell-penetrating peptides, Antimicrobial peptides, Perfluoropentanoic acid, Peptide quantitation, LC-MS

Introduction

Unprecedented progress has been made using monoclonal antibody (mAb)-based therapy in treating cancers. Particularly exciting are recent advances and remarkable clinical results in immunological checkpoint blockade and retargeting T cells via CAR T cells and bispecific antibodies [1–3]. Despite these tremendous successes, a vast majority of intracellular targets are not accessible for mAbs and CAR T cell therapy. Meanwhile, it is estimated that there are 3–4 times more intracellular targets than surface protein targets [4]. Since many of these proteins are not enzymes or surface receptors with readily druggable pockets, small molecules have largely been less effective in disrupting these large, shallow but topologically complex protein-protein interactions. Peptides, especially those capable of entering cells, represent a promising intermediate

molecular entity that can potentially harness the best characteristics of both small molecule therapeutics and large biologics to reach traditionally non-druggable intracellular targets.

Two large families of peptides have drawn extensive research attention during the past two decades. The first family is the so called cell-penetrating peptide (CPP) [5]. CPPs are generally short peptides (< 30 amino acids), often cationic and have the ability to not only penetrate cell membranes with little cytotoxicity to mammalian cells but also to ferry cargo (e.g., proteins, genes, or nanoparticles) into cells [6, 7]. Amino acid 48-60 (GRKKRRQRRRPPQ) from transactivator of transcription (TAT) protein of HIV-1 [8], penetratin (RQIKIWFQNRRMKWKKGG) derived from the amphiphilic *Drosophila* Antennapedia homeodomain [9], and polyarginine [10] (e.g., RRRRRRRR), among others, represent the early discovered and widely studied CPPs. They have been used as model systems in experiments designed to understand their internalization mechanism and cargo delivery capabilities [11, 12]. Over the years, more than 1500 natural/synthetic CPPs have been identified or designed, and a comprehensive list is available through database CPPsite 2.0 [13]. Many CPPs are now being explored in the preclinical space and a few are currently being evaluated in different phases of clinical trials as drug delivery vehicles [14]. Analysis of the CPP collections in database CPPsite 2.0 shows that more than 90% of them are cationic in nature, among which 64% have pI > 12 (Figure 1a). The extremely basic nature of these CPPs, such as (Arg)9, potentially enhances their cellular uptake efficiency, but creates an enormous challenge for their detection and analysis during drug discovery and development.

In addition to CPPs, another important category of extensively studied peptides bearing similar analytical challenges are cationic antimicrobial peptides (AMPs) [15, 16]. These peptides, as the name suggests, have ability to directly kill pathogenic microorganisms including bacteria, fungi, and viruses via selective membrane disruption or blocking intracellular functions. Some prominent AMP examples include polymyxin B and vancomycin, both of which are FDA-approved antibiotics. Many AMPs are being tested as an alternative treatment regime against the ever-growing number of multidrug-resistant infections [17]. Cationic AMPs share common characteristics of CPPs, like being strongly cationic and hydrophilic. Furthermore, certain AMPs can act as CPPs, and vice versa, some CPPs possess AMP properties. For example, the TAT peptide shows potent antibacterial activity against a broad spectrum of pathogens [18]. Phage display has identified two peptides that bind to heparan sulfate and block viral infection, and these AMPs were later found to internalize into cells [19, 20]. In total, more than 5000 AMPs have been identified up to date and multiple databases are publicly available [16, 21]. A plot of the collected AMPs indicates that more than 70% of them are basic and 14% among those have extreme pI > 12 (Figure 1b).

Basic and hydrophilic compounds are notoriously difficult to analyze in biological matrices because they are hard to extract, prone to nonspecific binding, and are not retained or show poor peak shapes under most chromatographic
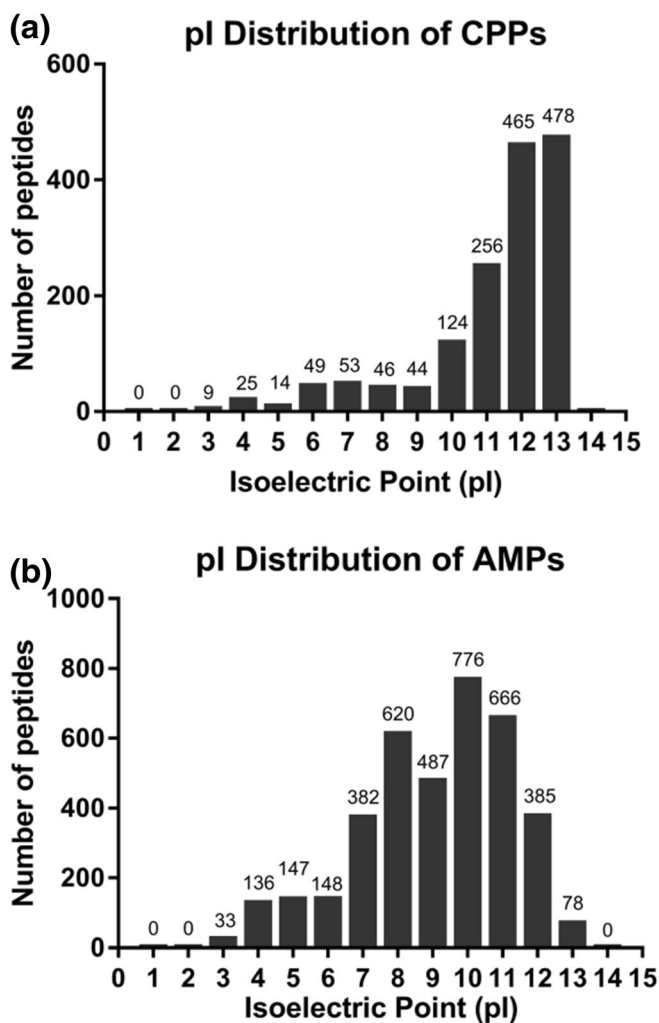

Figure 1. Isoelectric point (pI) distribution of (a) CPPs from database CPPsite2.0 and (b) AMPs from database LAMP

conditions. Therefore, exposure information is frequently missing from in vivo studies, which prevents an understanding of their pharmacokinetics/pharmacodynamics (PK/PD) relationship. Previous efforts to circumvent these obstacles have been by conjugating a fluorescent or radioactive tag to the peptides, so that cell entry, tissue distribution or pharmacokinetics could be monitored [22–24]. The drawback of these methods is that the conjugation might mask or modify the original properties of peptides and provide information not representative for the native peptides. These measurements may not necessarily reflect the real exposure of the intact peptides, thus limiting the value of PK/PD models or in vitro to in vivo correlations. A sensitive, selective and robust method to quantify these extremely positively charged peptides is required to accelerate the progression of new CPPs/AMPs into preclinical or clinical trials.

In this report, we describe a generic LC-MS–based quantitation method that employs perfluoropentanoic acid (PFPeA) as a mobile phase modifier to overcome the challenge of compound retention. We found that PFPeA, even at low μM concentration, offered an enormous benefit in retaining these

strongly basic peptides on reversed phase analytical columns. PFPeA also reduced the charge states of peptides and shifted the charge envelope to higher m/z values. Concentrations of PFPeA in the mobile phase were carefully evaluated to enable both good chromatographic separation and excellent MS sensitivity. We further demonstrated that a simple trichloroacetic acid (TCA) protein precipitation coupled with solid phase extraction (SPE) provided a robust way to extract these compounds from plasma and tissues. The overall extraction and LC-MS procedure offered an assay sensitivity of 1–5 ng/ml for the examined super cationic peptides. The developed method was successfully applied to directly measure peptide plasma stability and explore the pharmacokinetic profile and tissue distribution of these compounds without derivatization.

Experimental Section

Materials

Peptides R9, penetratin, nuclear localization signal (NLS), Bac2A, and TAT were purchased from Anaspec (Fremont, CA, USA). FHV Coat (35-49), HIV-1 Rev. (34-50), and HTLV-II Rex (4-16) were synthesized by Genscript (Piscataway, NJ, USA). G1 anti-HS peptide and G2 anti-3-OS HS peptide, perfluoropentanoic acid (PFPeA), trifloroacetic acid (TFA), dimethyl sulfoxide (DMSO), trichloroacetic acid (TCA), and Roche complete EDTA-free protease inhibitor cocktail (PIC) tablet were purchased from Sigma-Aldrich (Milwaukee, WI, USA). Mass spectrometry grade methanol, 0.1% formic acid (FA) in water and in acetonitrile (ACN), was obtained from Fisher Scientific (Pittsburgh, PA, USA). Oasis HLB and WCX 96-well μElution plates were purchased from Waters (Milford, MA, USA). Protein loBind 96-well plates were ordered from Eppendorf (Hamburg, Germany). Control rat plasma was purchased from Bioreclamation (Westbury, NY, USA). A liquid nitrogen compatible tissue pulverizer was purchased from Cellcrusher (Portland, OR, USA). Tenfold concentration (10 times) cell lysis buffer used for tissue extraction was ordered from Cell Signaling Technology (Danvers, MA, USA).

In Vivo Rat PK, Sample Collection, and Tissue Processing

All rats were housed in an AAALAC-accredited facility in accordance with USDA guidelines. The study was performed under a protocol approved by the local IACUC. In vivo studies were conducted using pre-cannulated male Wistar Han rats weighing between 0.31 and 0.33 kg. Rats were fasted with food removed approximately 16 h prior to dosing, and water provided ad libitum. TAT peptide was reconstituted in saline at 10 mg/ml and the formulation was administered at a dosing volume of 1 ml/kg via IV. Blood (0.25 ml) was sampled from jugular vein cannula at the following time points: 0, 2, 8, 15, and 30 min and 1, 2, 4, 7, 12, 18, and 24 h and was placed into EDTA tubes pre-spiked with complete PIC and the processed

plasma was stored at −70 °C until analysis. A duplicate set of rats were dosed and sacrificed 30 min post dose to collect the liver, kidney, heart, spleen, muscle, and brain. Collected tissues were immediately frozen on dry ice and homogenized manually using a tissue pulverizer cooled in liquid nitrogen on the day of sample analysis. One part of pulverized tissue by weight was mixed with three parts of lysis buffer (1x cell lysis buffer from cell signaling, 5 mM EDTA/EGTA, 1 tablet of PIC per 50 ml buffer) by volume and incubated at 4 °C for an hour.

Standards, Quality Control, and Sample Preparations

All compound stocks were prepared in DMSO at 1 mg/ml and stored at −20 °C when not in use. Plasma or tissue calibration standards and QCs were prepared in a 96-well protein low binding plate using an HP D300 Digital Liquid Dispenser (HP, Palo Alto, CA) to eliminate intermediate dilution steps and minimize potential losses due to non-specific binding from additional manipulations [25]. Plasma samples (the first five time points were 10 times diluted using blank plasma) or tissue homogenate were precipitated by adding 5% TCA in water (w/v) with internal standard (IS) at 1:4 ratio. Peptide G1 was used as IS at 100 ng/ml. After the plates were mixed and centrifuged at 4000×g for 10 min, the supernatant was removed and diluted with 400 μL water before proceeding to the automated SPE procedure using a Hamilton STAR liquid handling system (Reno, Nevada). In brief, the HLB μElution plate was washed with methanol and the resins were then equilibrated with water. After sample loading, the plate was washed twice with water before compound elution by 75% ACN/1% TFA. An equal volume of water was added to the elution plate before sample analysis. A similar procedure was applied for the WCX μElution plate, except that after sample loading, the plate was first washed by 2% NH$_4$OH then water before compound elution.

The stability of selected CPPs/AMPs peptides in rat EDTA or heparin plasma was determined by incubating the peptides in the plasma at 37 °C for the time period of 0–6 h. At each indicated time point, an aliquot was taken out from the master mix and quenched by adding four volumes of 5% TCA/IS. After the last time point, all samples were processed similarly as the in vivo plasma PK samples described above.

Sample Analysis by LC-MS

Liquid chromatography (LC) was carried out on a Waters ACQUITY UPLC *I*-class system (Waters, Milford, MA) with mobile phase A consisting of H$_2$O/0.1% FA, and mobile phase B of ACN/0.1% FA. PFPeA was added to both mobile phase A and B at concentrations indicated in the main text. Autosampler weak and strong wash solvents were H$_2$O/0.1% FA and 50% ACN/40% Isopropanol /10% acetone/0.05% FA, respectively. All compounds were analyzed on a Waters UPLC HSS T3 (2.1 × 50 mm, 1.8 μm) column maintained at 60 °C with gradient elution. The percentage of solvent A was held at 98% for 30 s while the sample was loaded to the column.

The organic phase was then ramped to 70% in 90 s and 95% after an additional 12 s then maintained at 95% for 18 s. The column was then flushed with two cycles of low to high organic solvent to minimize column carryover. The total run time for each injection was 3.8 min. All LC analyses had a flow rate of 0.75 ml/min.

Mass spectrometric detection was performed on an AB/Sciex 5500 or 6500 triple quadrupole system (Concord, ON, Canada) in the positive ion mode. All compounds were detected/quantified using their specific multiple reaction monitoring (MRM) transitions listed in Table S-2. Data was collected using Sciex Analyst 1.6.1 and processed by MultiQuant 3.0.1. Standard curves were fitted by a linear regression with $1/x^2$ weighting. The PK parameters were calculated using established non-compartmental model.

CPPs/AMPs Database Analysis and PI Calculation

CPP peptides were extracted from database CPPsite2.0 [13] (http://crdd.osdd.net/raghava/cppsite/). AMP collections were retrieved from database LAMP [21] (http://biotechlab.fudan.edu.cn/database/lamp/index.php). Peptide pI was calculated using an online tool [26] (http://isoelectric.org/). Hydrophobicity of peptides was calculated by summation of the relative hydrophobicity of each amino acid (Table S-1) using values published by Sereda et al. [27]. All graphs in the manuscript were prepared using Graphpad Prism 7 (La Jolla, CA, USA).

Results and Discussion

Peptide Retention Using PFPeA as a Mobile Phase Modifier

Liquid chromatography (LC) coupled with triple quadrupole mass spectrometry-based multiple reaction monitoring (MRM) is still the gold standard for sensitive and selective determination of drug quantitation in the pharmaceutical industry. A significant challenge of analyzing the majority of highly hydrophilic and positively charged CPPs and AMPs is their poor retention/recovery on most chromatographic columns. To facilitate the method development, we selected ten widely studied CPPs/AMPs as model analytes. These peptides have molecular weight ranging from 1400 to 2500 Da and their predicted pI are all above 12, except NLS (Table 1). The LC system and performance of a reversed phase column were calibrated using cytidine, labetalol, imipramine, and diclofenac, where the small hydrophilic cytidine eluted at 0.2 min and marked the column void volume (Figure 2). When the ten peptides were analyzed on the system, as expected, most were unretained and eluted at the column void volume due to their hydrophilicity (Figure 2). Based on their column behavior, the ten peptides were grouped into two categories. Type 1, including R9, TAT, G2, FHV, HIV-1, and HTLV, did not bind to the column at all and they all have a hydrophobicity score below − 1, while type 2 peptides (NLS, G1, Penetratin and Bac2A) showed split peaks eluting after 0.6 min with the major portion detected at the solvent front. Three out of four type 2 peptides have hydrophobicity above 2 and their retention on the column approximately correlated to their estimated hydrophobicity, even though the peak shape and reproducibility of the retained fractions fluctuated depending on the condition of the column, the LC system used and organic content in the sample.

To develop a reliable, MS-compatible LC method to analyze these types of peptides, we first explored HILIC and ion exchange–binding mechanisms. Both attempts failed owing to either peak broadening or no recovery. We then explored the possibility of using ion-pairing methods. Perfluorinated acids, such as TFA, have been frequently used as mobile phase additives for peptide and protein separation [28, 29]. We found that perfluoropentanoic acid (PFPeA) dramatically increased the retention of these peptides. Using an empirical concentration of 6 mM PFPeA (or 0.1%) in the mobile phases, all peptides eluted between 1.5 and 1.8 min as a single sharp and symmetrical peak (Figure 2). PFPeA can in fact sufficiently

Table 1. Sequences and Chemical Properties of Selected CPPs and AMPs

Type	Peptide	Sequence	MW (Da)	pI	Hydrophobicity[h]	CPP	AMP
1	R9	RRRRRRRRR	1423.7	12.7	−2.34	√	
1	TAT [a]	GRKKRRQRRRPPQ	1719.0	12.5	−3.12	√	√
1	G2 [b]	MPRRRIRRRQK	1709.1	12.6	−1.09	√	√
1	FHV [c]	RRRRNRTRRNRRRVR	2164.5	12.8	−2.76	√	
1	HIV-1 [d]	TRQARRNRRRRWRERQR	2437.8	12.4	−1.67	√	
1	HTLV [e]	TRRQRTRRARRNR	1783.0	12.7	−2.07	√	
2	NLS [f]	PKKKRKVEDPYC	1490.8	8.9	−0.96	√	
2	G1 [b]	LRSRTKIIRIRH	1548.9	12.3	2.23	√	√
2	Penetratin	RQIKIWFQNRRMKWKKGG	2360.9	12.1	2.31	√	√
2	Bac2A [g]	RLARIVVIRVAR	1421.8	12.3	3.69		√

[a]Derived from HIV-1 TAT protein residue 48–60
[b]Anti-heparan sulfate peptide group 1 (G1) and group 2 (G2) identified by phage display
[c]Derived from Flock house virus (FHV) coat protein residue 35–49
[d]Derived from HIV-1 Rev. protein residue 34–50
[e]Derived from Human T cell leukemia virus type 2 (HTLV-2) Rex protein residue 4–16
[f]Nuclear localization signal derived from SV 40
[g]Bac2A: a linear variant of cationic antimicrobial peptide bactenecin found in bovine neutrophils
[h]Hydrophobicity of peptides was calculated by summation of the relative hydrophobicity of each amino acid (Table S-1) using values published by Sereda et al. [27]
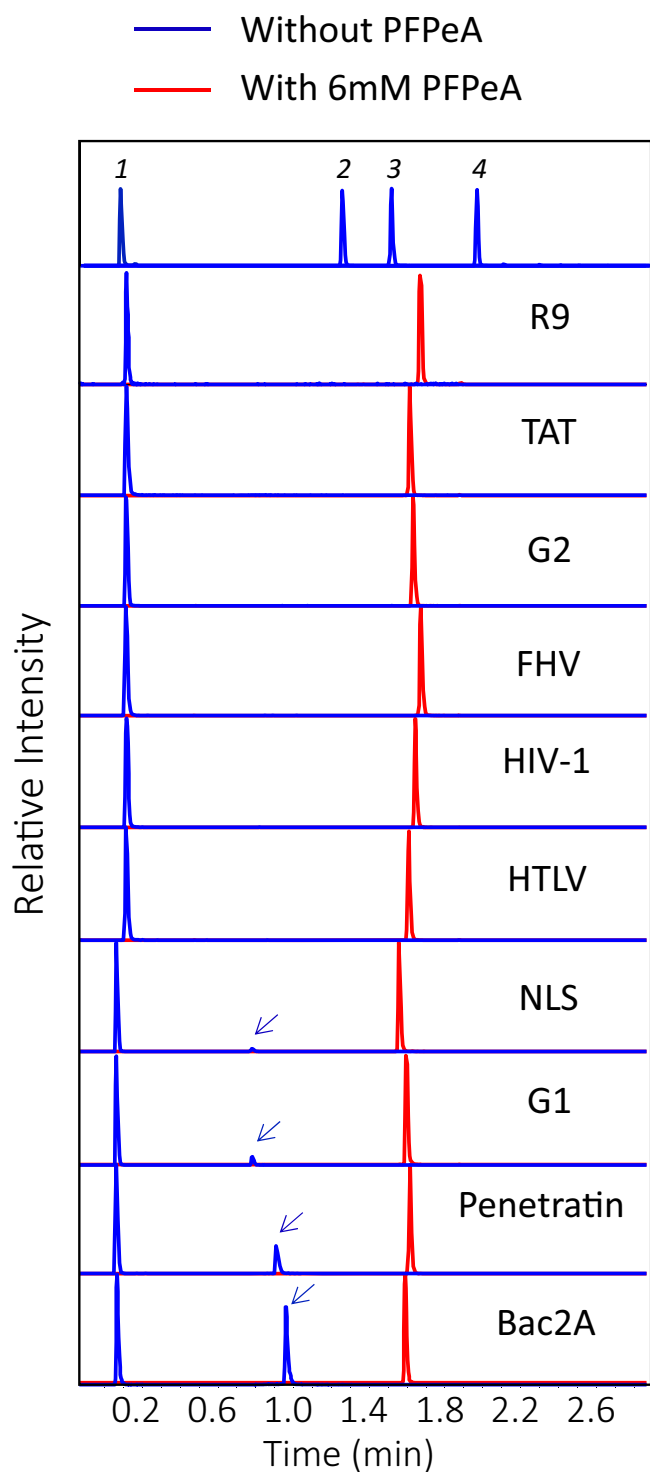
Figure 2. PFPeA facilitates the binding of extremely positively charged peptides on reversed phase columns. Performance of the column was tested using cytidine (*1*), labetalol (*2*), imipramine (*3*) and diclofenac (*4*). Retained fraction of NLS, G1, Penetratin and Bac2A was labeled by an arrow

alter the peptides' apparent hydrophobicity and separate them from the solvent front. This observation laid the foundation for us to develop a fast, sensitive, and robust LC-MS–based quantitation method.

MRM Setup and Charge Stripping by PFPeA

To establish MRM methods, each peptide in 50% ACN/0.1% FA was infused into the mass spectrometer and corresponding parent and daughter ion pairs were identified. Due to the number of basic amino acids in the sequences of the peptide test set, the most abundant parent ions usually carried more than 4 charges and fell in the 200–400 *m/z* range (Figure 3 and S-1). During the MRM optimization process, we observed that adding PFPeA to the neat solution reduced the peptides' charge state. For example, the dominant charge state of R9 without PFPeA was + 6. When the PFPeA concentration was added at 0.5 mM, the major R9 charge state was reduced to + 4 and at 2 mM PFPeA, the dominant charge state was + 3 and an abundant peak of + 2 could also be detected (Figure 3a). Similarly, the dominant charge state of TAT without PFPeA was + 5 which was reduced to + 4 at 0.5 mM and + 3 at 2 mM PFPeA (Figure 3b). This charge stripping phenomenon was observed for all the other peptides (Figure S-1) and allowed us to select MRM at higher *m/z* range with potentially less interference from co-eluting ions. Thus, each peptide was also infused at 0.5–2 mM PFPeA to cover the lower charge states, and MRM for each observed relatively abundant product ion from each charge state was monitored during the initial method development phase. Details for the MRM methodology were included in Table S-2. Addition of PFPeA in the infusion solution sometimes created additional ion peaks due to apparent adduct formation, such as seen in Figure 3b middle panel (*m/z* range 450–850). Increasing the declustering potential of the orifice and the desolvation gas flow of the Sciex Turbo V ion source generally decreased the presence of these adducts.

Manipulating the charge envelope of peptides/proteins has been tested for various purposes by applying supercharging reagents [30], chemical derivatization [31], solvent or gas phase ion/ion reaction, or proton transfer [32]. PFPeA-induced charge stripping could potentially involve the ion pairing effect of the perfluorinated anions that mask the basic groups on the peptides for protonation or PFPeA lowered surface tension (PFPeA ∼ 16 dyn/cm vs. H2O ∼ 72 dyn/cm) of the electrospray droplet thus decreasing the charge density before droplet fission or the combination of both.

Assay Optimization by Fine Tuning PFPeA Concentration

A major concern of using ion pairing reagents in a mass spectrometer is their potential ion suppression effect on the analytes and possible deterioration of instrument performance at high concentration. To evaluate and fine tune the influence of PFPeA on signal response and instrument performance, we titrated PFPeA in the mobile phase from 1 μM to 10 mM. The MRM responses from the two most sensitive charge states were presented for each peptide in Figure 4 and Figure S-2. All peptides exhibited a bell shape signal response with increasing PFPeA concentration. Interestingly, the most sensitive charge state of type 1 peptides, such as R9, TAT, and G2, all reached maximal signal response at
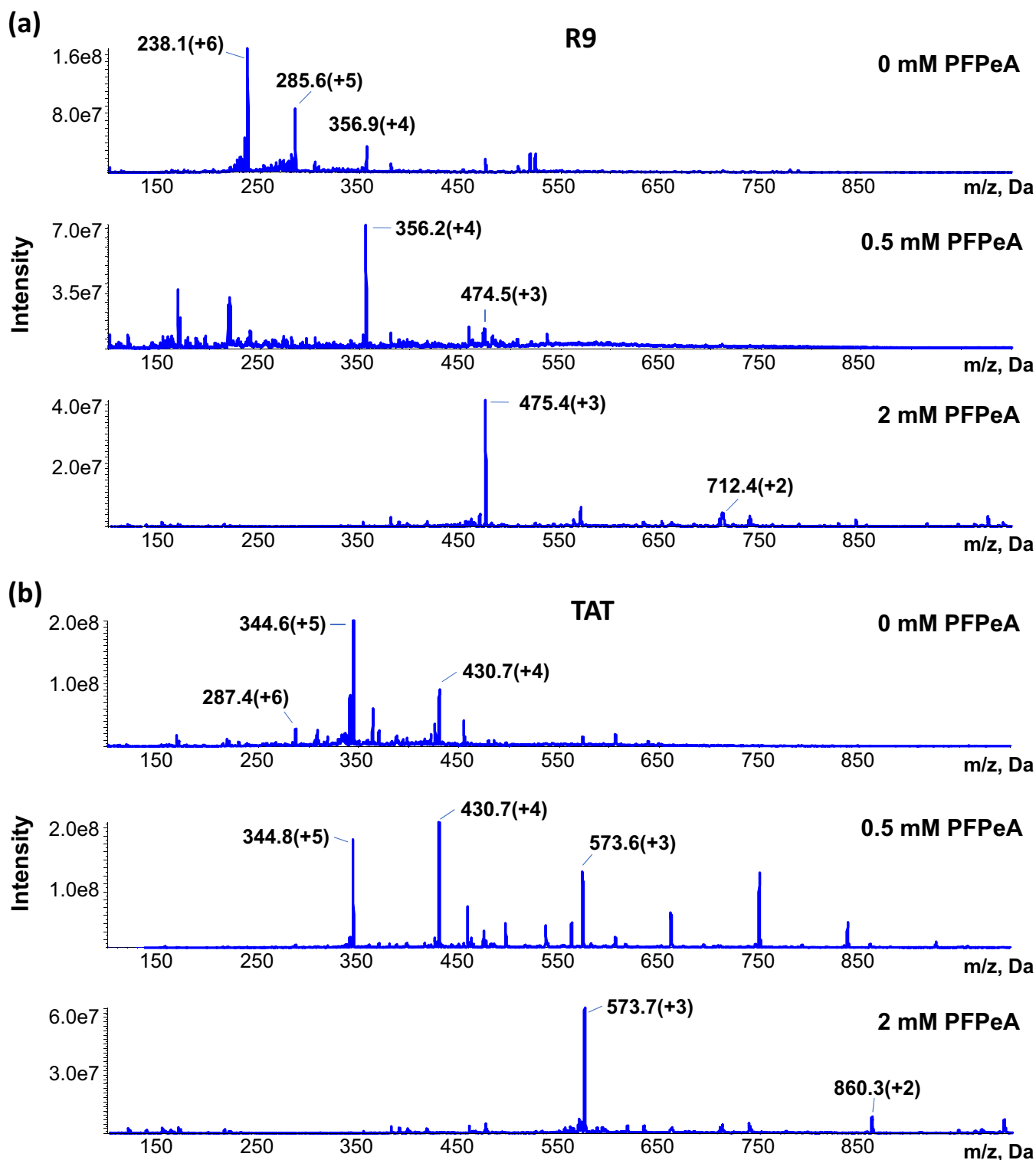
Figure 3. Increased PFPeA concentration reduces peptides' charge state. (**a**) Effect of PFPeA concentrations on R9 charge distribution; (**b**) effect of PFPeA concentrations on TAT charge distribution

approximately 0.1 mM PFPeA with minimal differences in signal intensity between 0.05 and 0.5 mM. Additionally, all type 1 peptides were well retained on the column at 0.1 mM concentration and eluted after 1.2 min (Figure S-3). Thus, this concentration (0.1 mM or 0.0015%) was selected to

analyze this class of peptides. On the other hand, the most sensitive charge state for type 2 peptides (G1, Penetratin, Bac2A, and NLS) reached maximal signal intensity at approximately 10 μM PFPeA and the signal declined sharply with increasing PFPeA concentration. Fortunately, even

with 10 μM PFPeA, these peptides were well retained on column and eluted after 0.8 min with excellent peak shape and consistency (Figure S-3). Therefore, 10 μM or 0.00015% PFPeA was chosen to analyze type 2 peptides.

The low PFPeA concentration required in the mobile phase to achieve consistent retention for these peptides was unanticipated. Other perfluorinated acids, such as TFA (0.1% or 13.1 mM) and pentafluoropropionic acid (10–50 mM), have been routinely used as mobile phase additives at much higher empirical concentrations to improve peptide/protein peak shapes [33, 34]. When UV is used as a detection method, high concentration of ion-pairing reagents has no significant effect on the signal as they are UV transparent. However, when a similar LC condition is adapted to MS detection, severe ion suppression is frequently observed which limits its applicability, especially when alternative methods, such as HILIC, are available. Here, we demonstrated that a very low concentration of PFPeA was sufficient to achieve good retention, peak shape and sensitivity for these strongly basic peptides. Rather than the ion suppression observed at high PFPeA concentrations, this low PFPeA addition allowed elution of the peptides at higher organic mobile phase composition, thus ensuring good ionization and enhanced overall MS signals. Thus, it is important to optimize the concentration of ion-pairing reagents to achieve the necessary chromatographic retention and MS sensitivity. The workflow demonstrated here can be adopted for these evaluations.

Efficient Sample Extraction by TCA Protein Precipitation Coupled with SPE

Sample preparation and compound extraction play a critical role with respect to achieving assay sensitivity and robustness. Immunoprecipitation using a peptide-specific antibody would be an ideal approach for enriching the analyte and eliminating interferences [35]. However, in the discovery phase, a large variety of different peptides are encountered and it is cost and time prohibitive to raise an antibody against each individual candidate. Additionally, immune responses against these small peptides are not entirely predictable. Therefore, we explored alternative strategies, such as protein precipitation and solid-phase extraction (SPE), as more generic and applicable sample purification approaches. We found that 5% trichloroacetic acid (TCA, *w/v*) can efficiently remove the majority of plasma/tissue proteins while keeping the strongly basic peptides in the supernatant. Thus, this was chosen as the first step in sample cleanup. To eliminate the potential effect of TCA on column performance, we then evaluated weak cation exchange mixed mode SPE (WCX) and hydrophilic-lipophilic balanced (HLB) SPE μElution plates to remove TCA from the supernatant. It appeared that HLB performed slightly better than WCX, and the overall recovery of compounds spiked in plasma after HLB for R9, TAT, G2, FHV, HIV-1, HTLV, and NLS was 58%, 67%, 48%, 55%, 32%, 53% and 44%, respectively. A similar recovery from different types of tissues was also observed. Consequently, 5% TCA protein precipitation coupled with HLB SPE was chosen as the final sample preparation method and G1 was used as the internal standard (IS).

Penetratin and Bac2A from the type 2 peptides are more hydrophobic compared with the others. Recovery of these two after TCA precipitation was low (< 10%) and an alternative extraction method was developed for this type of peptides which will be reported separately.
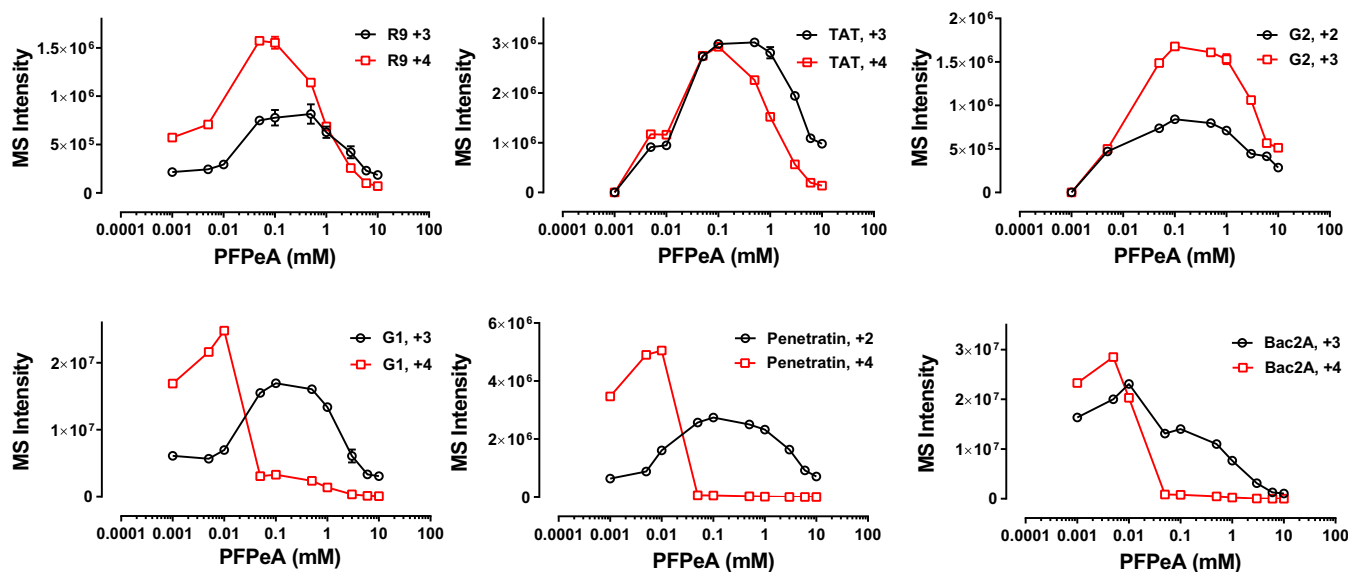
Figure 4. Effect of PFPeA concentration on MRM sensitivity of the two most prominent charge states as indicated on each panel. PFPeA concentrations were 0.001, 0.005, 0.01, 0.05, 0.1, 0.5, 1, 3, 6, 10 mM. The + 3 charge state of penetratin has a similar profile of intensity vs. PFPeA concentration to the + 4 charge state but with an overall lower intensity that is similar to the + 2 charge state, so the + 2 and + 4 charge states were chosen to show the representative profiles

Table 2. Standard Curve Precision and Accuracy ($n = 5$). Accuracy Is Expressed as [(Mean Observed Concentration) / (Nominal Concentration)] × 100 (%). CV Is Coefficient of Variation of Back Calculated Concentration. Among the Five Replicates, the Minimal R-squared (R^2) After Standard Curve Linear Regression Is 0.991, 0.992, 0.991, and 0.981 for R9, TAT, HTLV, and NLS, respectively

| Standard (ng/ml)	R9		TAT		HTLV		NLS	
	Accuracy (%)	%CV	Accuracy (%)	%CV	Accuracy (%)	%CV	Accuracy (%)	%CV
1.00	–	–	102	7.18	102	7.11	98.8	8.25
2.00	104	5.29	99.4	10.8	99.8	14.7	100	7.83
5.00	92.5	14.0	101	7.09	87.4	13.9	110	9.57
10.0	97.2	8.98	88.3	4.62	100	2.27	86.3	12.8
50.0	92.8	4.44	110	8.57	101	4.07	86.4	8.07
200	93.4	5.24	106	5.80	98.6	5.78	88.7	7.24
500	99.6	5.13	104	2.51	101	5.00	97.4	5.04
1000	101	2.86	99.3	3.36	103	2.97	108	3.99
2000	119	4.17	91.0	2.14	101	2.61	119	5.11

Method Performance

The overall assay performance was qualified for the purpose of discovery screening. For most peptides, a sensitivity of 1 ng/ml could be reached from 50 µl plasma (Table 2, S-3 and Figure S-4). All standard curves demonstrated acceptable accuracy (< 20%) and precision (< 20%) (Table 2 and Table S-3) with acceptable peaks at lower limit of quantitation (LLOQ) (Figure S-4). If the intended application is for GLP or clinical studies, a full validation following the ICH guidance (https://www.ich.org/fileadmin/Public_Web_Site/ICH_Products/Guidelines/Multidisciplinary/M10/M10EWG_Step2_DraftGuideline_2019_0226.pdf) should be completed and this work could be the foundation for more thorough validations to align with the additional regulation requirements.

Basic compounds are notoriously sticky and generally exhibit high carryover during analysis. To eliminate column carryover, two extra on-column wash cycles were added to the LC gradient (refer to "Method" section). In other words, after analyte elution, flushing the column with two rapid gradients of a low to high percentage of mobile phase B within a run allowed efficient removal of column carryover. Even with these extra wash cycles, the total run time was still less than 4 min to ensure reasonable throughput. Carryover for TAT, G2, HIV-1, HTLV, and NLS was less than 0.05% and carryover for R9 and FHV was less than 0.5%. Occasionally, carryover could come from the specific autosampler system used; we found adding low mM of PFPeA to the wash solvents helped decrease the autosampler carryover. Since the PFPeA concentration used in the mobile phases was particularly low, no apparent
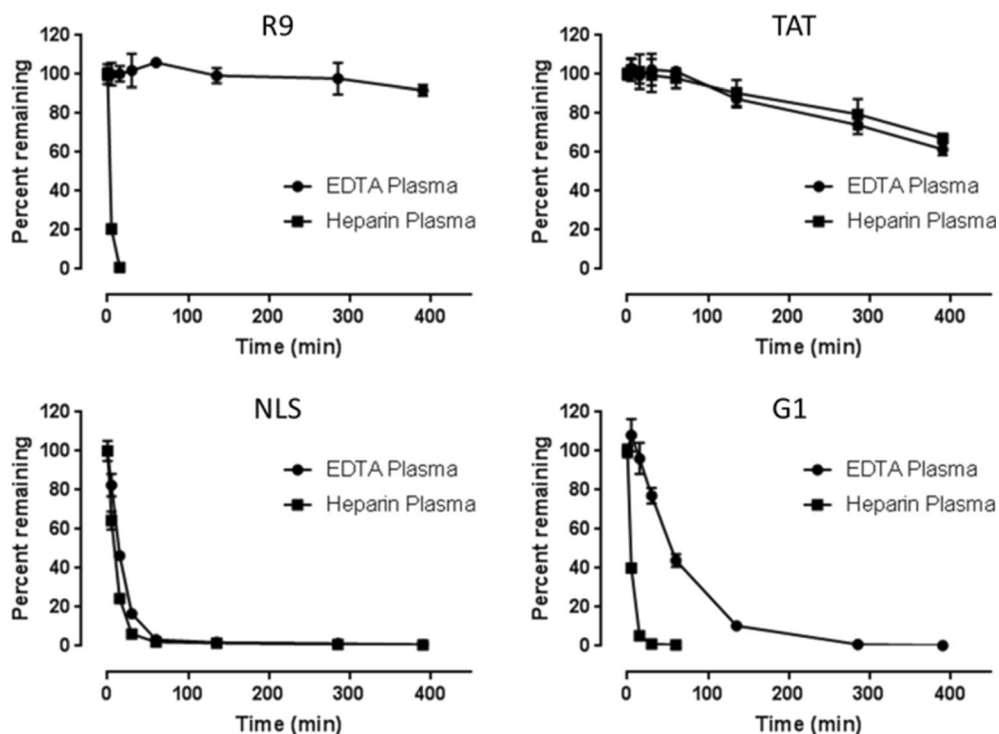
Figure 5. Plasma stability of selected peptides. The time points are 0, 5, 15, 30, 60, 135, 285, and 390 min. Error bar represents the standard deviation from experiments conducted in triplicate
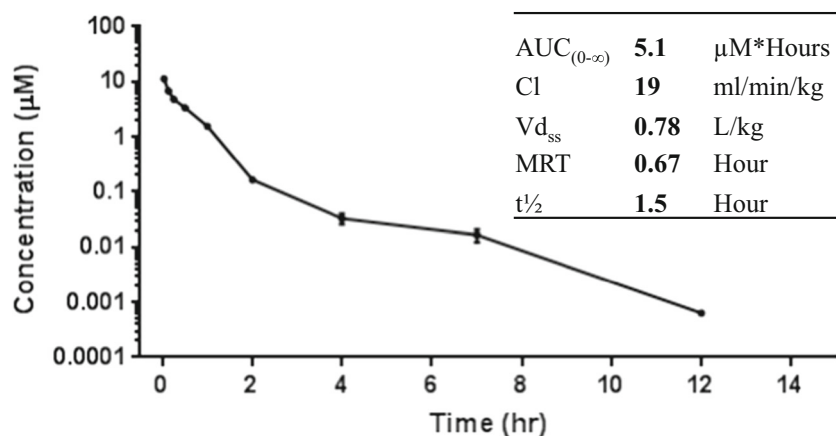
Figure 6. Plasma pharmacokinetic profile of TAT following an IV bolus administration at 10 mg/kg in rat. Data represents mean concentration with standard deviation ($n = 3$)

MS performance deterioration was observed after prolonged routine use.

Evaluating Plasma Stability of Selected CPPs/AMPs

In order for CPPs/AMPs to reach and enter the target cells either as a drug delivery vehicle or as a therapeutic agent, they must show adequate exposure in the systemic circulation. Most techniques used to detect these peptides rely on fluorophore conjugation or other labeling methods and are not able to distinguish between intact labeled molecules and their degradation products which can complicate the interpretation of results [36].

To demonstrate the feasibility of our established quantitation method, we first applied it to evaluate the plasma stability of selected CPPs/AMPs. Results for R9, TAT, NLS, and G1 in both EDTA plasma and heparin plasma are shown in Figure 5. The peptide R9 was relatively stable in EDTA plasma while 80% was degraded in heparin plasma within 5 min. No clear stability difference in the two types of plasma was observed for TAT as well as NLS; however, TAT was reasonably stable with an apparent half-life of more than 6 h while NLS degraded quickly with an approximate half-life of 10 min in either EDTA or heparin plasma. The G1 peptide was less susceptible to protease activity in EDTA plasma compared with heparin plasma with an estimated half-life of 51 and 3.7 min, respectively.

EDTA and heparin are two frequently used anticoagulants. EDTA is also an effective pleotropic metalloprotease inhibitor. Heparin resembles the highly negatively charged glycosaminoglycans found on cell surface proteoglycans, which is believed to provide binding sites for certain CPPs/AMPs for endocytosis [37]. Even though the selected CPPs/AMPs are all highly basic, their degradation pathways are clearly distinct from each other, and plasma collection method (EDTA or heparin) may dramatically affect their stability post sample collection. EDTA can completely inhibit the enzymes that degrade R9 and slow down the degradation of G1, but almost has no inhibitory effect on the TAT and NLS protease(s). The highly negative charged heparin added in plasma may interact with the positively charged peptides and potentially stabilize the peptides. The result shown in Figure 5 does not support this hypothesis and heparin does not have any influence on the stability of the four peptides compared with EDTA. Either the peptides do not bind to heparin or the binding is weak providing negligible stabilization effect.

Different strategies have been reported to improve peptide stability, including using more stable D enantiomers or non-natural amino acids [38], backbone cyclization or stapling [39], or stabilization through β- or γ-peptoids [40]. Compared with other fluorescence-based techniques, our method can provide a direct measurement of the intact peptides and help with peptide stability screening and structure optimization without requiring labeling steps.

PK and Tissue Distribution of TAT

Considering the relative stability of TAT in rat plasma, we further applied the method to examine its plasma pharmacokinetics after IV administration. The time-dependent concentration curve is shown in Figure 6. The assay LLOQ at 1 ng/ml allowed us to capture the elimination phase appropriately. TAT showed a relatively fast plasma clearance of 19 ml/min/kg and small volume of distribution (Vdss) of 0.78 L/kg. The terminal

Table 3. Tissue Distribution of the Intact TAT Peptide 30 min After IV Administration. Data Represents Average Concentration ± Standard Deviation from Three Animals. Tissue Molar Concentration Was Calculated Assuming Tissue Density of 1 g/ml

Concentration	Tissue						
	Liver	Heart	Kidney	Spleen	Muscle	Brain	Plasma
mg/kg (μM)	1.7 ± 0.3 (1.0 ± 0.2)	2.7 ± 1.2 (1.6 ± 0.7)	0.06 ± 0.01 (0.04 ± 0.01)	0.16 ± 0.07 (0.09 ± 0.04)	0.46 ± 0.12 (0.27 ± 0.07)	0.03 ± 0.02 (0.02 ± 0.01)	- (3.4 ± 0.3)

half-life was determined to be 1.5 h with a mean resonance time (MRT) of 0.67 h. To evaluate its biodistribution after systemic administration, liver, heart, spleen, kidney, muscle, and brain were dissected 30 min post-dosing. Exposure of the intact TAT peptide was determined and summarized in Table 3. A broad tissue distribution was observed with liver and heart having the most exposure representing 44% of the dose. An encouraging observation is that a detectable level of TAT was also observed in the brain, even though the overall brain concentration represents only 0.6% of plasma exposure.

Previously, TAT tissue distribution was assessed using a heavy metal conjugated version where most of the tissue uptake was found in the liver and kidney based on the amount of radioactivity accumulated [23]. Since it is not clear to which degree the distribution of radioactivity reflects the characteristics of the intact peptide or metabolites, an explicit data explanation is difficult. Our LC-MS–based native peptide analysis enabled us for the first time to directly quantify intact TAT from biological matrices and evaluate its pharmacokinetics and biodistribution.

Conclusions

Substantial efforts are being directed toward understanding the mechanism of cell entry for CPPs/AMPs and exploring their potential application in the cancer drug delivery, disease diagnosis, and treatment. Considering a large portion of CPPs/AMPs are highly positively charged and hydrophilic, we developed and optimized a generic LC-MS/MS method using PFPeA as a mobile phase modifier to address the challenges associated with analyzing extremely basic peptides. The low concentration of PFPeA used in the LC system offers excellent peptide retention and overcomes the common drawbacks of ion suppression and instrument contamination. The sample preparation by SPE provides reasonable compound recovery, and is generic and high throughput. The overall method is accurate and precise. It allows us to screen the plasma stability of these highly cationic peptides or their derivatives. It also allows us to evaluate their PK profiles and biodistribution of the parent drug. Finally, the presented method provides a foundation for the field to quantitatively understand compound biodistribution and establish PK/PD relationships.

Acknowledgements

The authors gratefully acknowledge Scott E. Fauty and the Biochemical Toxicology & Toxicokinetics group in Merck & Co., Inc. (West Point, PA, USA) for conducting the in vivo PK experiment. We thank Drs. Christine Fandozzi, Kevin Bateman, Vincenzo Pucci, Rena Zhang, Raymond Evers and Jerome Hochman for insightful discussions.

Compliance with Ethical Standards

Conflict of Interest The authors were employed by Merck Sharp & Dohme Corp., a subsidiary of Merck & Co., Inc., Kenilworth, NJ, USA, during the work described in this article. The authors declare no competing financial interest.

References

1. Weiner, G.J.: Building better monoclonal antibody-based therapeutics. Nat. Rev. Cancer. **15**, 361–370 (2015)
2. Garon, E.B., Rizvi, N.A., Hui, R., Leighl, N., Balmanoukian, A.S., Eder, J.P., Patnaik, A., Aggarwal, C., Gubens, M., Horn, L., Carcereny, E., Ahn, M.J., Felip, E., Lee, J.S., Hellmann, M.D., Hamid, O., Goldman, J.W., Soria, J.C., Dolled-Filhart, M., Rutledge, R.Z., Zhang, J., Lunceford, J.K., Rangwala, R., Lubiniecki, G.M., Roach, C., Emancipator, K., Gandhi, L., Investigators, K.: Pembrolizumab for the treatment of non-small-cell lung cancer. N. Engl. J. Med. **372**, 2018–2028 (2015)
3. June, C.H., Sadelain, M.: Chimeric antigen receptor therapy. N. Engl. J. Med. **379**, 64–73 (2018)
4. Miersch, S., Sidhu, S.S.: Intracellular targeting with engineered proteins. F1000Res. **5**, (2016)
5. Koren, E., Torchilin, V.P.: Cell-penetrating peptides: breaking through to the other side. Trends Mol. Med. **18**, 385–393 (2012)
6. Raucher, D., Ryu, J.S.: Cell-penetrating peptides: strategies for anticancer treatment. Trends Mol. Med. **21**, 560–570 (2015)
7. Reissmann, S.: Cell penetration: scope and limitations by the application of cell-penetrating peptides. J. Pept. Sci. **20**, 760–784 (2014)
8. Vives, E., Brodin, P., Lebleu, B.: A truncated HIV-1 Tat protein basic domain rapidly translocates through the plasma membrane and accumulates in the cell nucleus. J. Biol. Chem. **272**, 16010–16017 (1997)
9. Derossi, D., Joliot, A.H., Chassaing, G., Prochiantz, A.: The third helix of the Antennapedia homeodomain translocates through biological membranes. J. Biol. Chem. **269**, 10444–10450 (1994)
10. Matsushita, M., Tomizawa, K., Moriwaki, A., Li, S.T., Terada, H., Matsui, H.: A high-efficiency protein transduction system demonstrating the role of PKA in long-lasting long-term potentiation. J. Neurosci. **21**, 6000–6007 (2001)
11. Madani, F., Lindberg, S., Langel, U., Futaki, S., Graslund, A.: Mechanisms of cellular uptake of cell-penetrating peptides. J Biophys. **2011**, 414729 (2011)
12. Trabulo, S., Cardoso, A.L., Mano, M., De Lima, M.C.: Cell-penetrating peptides-mechanisms of cellular uptake and generation of delivery systems. Pharmaceuticals (Basel). **3**, 961–993 (2010)
13. Agrawal, P., Bhalla, S., Usmani, S.S., Singh, S., Chaudhary, K., Raghava, G.P., Gautam, A.: CPPsite 2.0: a repository of experimentally validated cell-penetrating peptides. Nucleic Acids Res. **44**, D1098–D1103 (2016)
14. Guidotti, G., Brambilla, L., Rossi, D.: Cell-penetrating peptides: from basic research to clinics. Trends Pharmacol. Sci. **38**, 406–424 (2017)
15. Zhang, L.J., Gallo, R.L.: Antimicrobial peptides. Curr. Biol. **26**, R14–R19 (2016)
16. Wang, G., Li, X., Wang, Z.: APD3: the antimicrobial peptide database as a tool for research and education. Nucleic Acids Res. **44**, D1087–D1093 (2016)
17. Gordon, Y.J., Romanowski, E.G., McDermott, A.M.: A review of antimicrobial peptides and their therapeutic potential as anti-infective drugs. Curr. Eye Res. **30**, 505–515 (2005)
18. Zhu, W.L., Shin, S.Y.: Effects of dimerization of the cell-penetrating peptide tat analog on antimicrobial activity and mechanism of bactericidal action. J. Pept. Sci. **15**, 345–352 (2009)
19. Tiwari, V., Liu, J., Valyi-Nagy, T., Shukla, D.: Anti-heparan sulfate peptides that block herpes simplex virus infection in vivo. J. Biol. Chem. **286**, 25406–25415 (2011)
20. Parn, K., Eriste, E., Langel, U.: The antimicrobial and antiviral applications of cell-penetrating peptides. Methods Mol. Biol. **1324**, 223–245 (2015)
21. Zhao, X., Wu, H., Lu, H., Li, G., Huang, Q.: LAMP: a database linking antimicrobial peptides. PLoS One. **8**, e66557 (2013)
22. Ramaker, K., Henkel, M., Krause, T., Rockendorf, N., Frey, A.: Cell penetrating peptides: a comparative transport analysis for 474 sequence motifs. Drug Deliv. **25**, 928–937 (2018)
23. Sarko, D., Beijer, B., Garcia Boy, R., Nothelfer, E.M., Leotta, K., Eisenhut, M., Altmann, A., Haberkorn, U., Mier, W.: The pharmacokinetics of cell-penetrating peptides. Mol. Pharm. **7**, 2224–2231 (2010)

24. Edwards, A.B., Cross, J.L., Anderton, R.S., Knuckey, N.W., Meloni, B.P.: Poly-arginine R18 and R18D (D-enantiomer) peptides reduce infarct volume and improves behavioural outcomes following perinatal hypoxic-ischaemic encephalopathy in the P7 rat. Mol Brain. **11**, 8 (2018)

25. Roselle, C., Whitehouse, D., Follmer, T., Ansbro, F., Bouaraphan, S., Guan, L., Wang, S.K., Shank-Retzlaff, M., Verch, T.: Evaluation of a digital dispenser for direct curve dilutions in a vaccine potency assay. J. Immunol. Methods. **442**, 20–28 (2017)

26. Kozlowski, L.P.: IPC - isoelectric point calculator. Biol. Direct. **11**, 55 (2016)

27. Sereda, T.J., Mant, C.T., Sonnichsen, F.D., Hodges, R.S.: Reversed-phase chromatography of synthetic amphipathic alpha-helical peptides as a model for ligand/receptor interactions. Effect of changing hydrophobic environment on the relative hydrophilicity/hydrophobicity of amino acid side-chains. J. Chromatogr. A. **676**, 139–153 (1994)

28. Pearson, J.D., McCroskey, M.C.: Perfluorinated acid alternatives to trifluoroacetic acid for reversed-phase high-performance liquid chromatography. J. Chromatogr. A. **746**, 277–281 (1996)

29. Shibue, M., Mant, C.T., Hodges, R.S.: Effect of anionic ion-pairing reagent hydrophobicity on selectivity of peptide separations by reversed-phase liquid chromatography. J. Chromatogr. A. **1080**, 68–75 (2005)

30. Iavarone, A.T., Williams, E.R.: Mechanism of charging and supercharging molecules in electrospray ionization. J. Am. Chem. Soc. **125**, 2319–2327 (2003)

31. Krusemark, C.J., Frey, B.L., Belshaw, P.J., Smith, L.M.: Modifying the charge state distribution of proteins in electrospray ionization mass spectrometry by chemical derivatization. J. Am. Soc. Mass Spectrom. **20**, 1617–1625 (2009)

32. Pitteri, S.J., McLuckey, S.A.: Recent developments in the ion/ion chemistry of high-mass multiply charged ions. Mass Spectrom. Rev. **24**, 931–958 (2005)

33. Shibue, M., Mant, C.T., Hodges, R.S.: Effect of anionic ion-pairing reagent concentration (1-60 mM) on reversed-phase liquid chromatography elution behaviour of peptides. J. Chromatogr. A. **1080**, 58–67 (2005)

34. Flieger, J.: Application of perfluorinated acids as ion-pairing reagents for reversed-phase chromatography and retention-hydrophobicity relationships studies of selected beta-blockers. J. Chromatogr. A. **1217**, 540–549 (2010)

35. Xu, Y., Sun, L., Anderson, M., Belanger, P., Trinh, V., Lavallee, P., Kantesaria, B., Marcoux, M.J., Breidinger, S., Bateman, K.P., Goykhman, D., Woolf, E.J.: Insulin glargine and its two active metabolites: a sensitive (16pM) and robust simultaneous hybrid assay coupling immunoaffinity purification with LC-MS/MS to support biosimilar clinical studies. J. Chromatogr. B Anal. Technol. Biomed. Life Sci. **1063**, 50–59 (2017)

36. Herbig, M.E., Weller, K.M., Merkle, H.P.: Reviewing biophysical and cell biological methodologies in cell-penetrating peptide (CPP) research. Crit. Rev. Ther. Drug Carrier Syst. **24**, 203–255 (2007)

37. Rizzuti, M., Nizzardo, M., Zanetta, C., Ramirez, A., Corti, S.: Therapeutic applications of the cell-penetrating HIV-1 tat peptide. Drug Discov. Today. **20**, 76–85 (2015)

38. Verdurmen, W.P., Bovee-Geurts, P.H., Wadhwani, P., Ulrich, A.S., Hallbrink, M., van Kuppevelt, T.H., Brock, R.: Preferential uptake of L-versus D-amino acid cell-penetrating peptides in a cell type-dependent manner. Chem. Biol. **18**, 1000–1010 (2011)

39. Reichart, F., Horn, M., Neundorf, I.: Cyclization of a cell-penetrating peptide via click-chemistry increases proteolytic resistance and improves drug delivery. J. Pept. Sci. **22**, 421–426 (2016)

40. Jing, X., Yang, M., Kasimova, M.R., Malmsten, M., Franzyk, H., Jorgensen, L., Foged, C., Nielsen, H.M.: Membrane adsorption and binding, cellular uptake and cytotoxicity of cell-penetrating peptidomimetics with alpha-peptide/beta-peptoid backbone: effects of hydrogen bonding and alpha-chirality in the beta-peptoid residues. Biochim. Biophys. Acta. **1818**, 2660–2668 (2012)